Journal of Magnetic Resonance **147,** 170–178 (2000)
doi:10.1006/jmre.2000.2191, available online at http://www.idealibrary.com on IDEAL®

Dipolar Coupling Information in Multispin Systems: Application of a Compensated REDOR NMR Approach to Inorganic Phosphates

Jerry C. C. Chan and Hellmut Eckert[1]

Institut für Physikalische Chemie, Westfälische Wilhelms-Universität Münster, Schlossplatz 7, D48149 Münster, Germany

Received February 28, 2000; revised August 11, 2000

An experimental strategy has been developed for measuring multiple dipole–dipole interactions in inorganic compounds using the technique of rotational echo double resonance (REDOR) NMR. Geometry-independent information about the dipole couplings between the observe nuclear species S (arbitrary quantum number) and the heteronuclear species I (spin-$\frac{1}{2}$) can be conveniently obtained from the experimental curve of $\Delta S/S_0$ versus dipolar evolution time by limiting the analysis to the initial data range $0 < \Delta S/S_0 < 0.30$. Numerical simulations have been carried out on a three-spin system of type SI_2 in order to assess the effect of the I–I homonuclear dipole–dipole coupling and the influence of experimental imperfections such as finite pulse length and misadjustments of the 180° pulses applied to the I-spin species. The simulations show further that within the initial data range the effects of such misadjustments can be internally compensated by a modified sequence having an additional 180° pulse on the I channel in the middle of the dipolar evolution periods. Experimental $^{27}Al\{^{31}P\}$ REDOR results on the multispin systems $Al(PO_3)_3$, $AlPO_4$, $[AlPO_4]_{12}(C_3H_7)_4NF$, and Na_3PO_4 confirm the general utility of this approach. Thus, for applications to unknown systems the compensation strategy obviates calibration procedures with model compounds. © 2000 Academic Press

Key Words: **REDOR; heteronuclear dipole–dipole interaction; MAS; second moment; phosphates.**

INTRODUCTION

The technique of rotational echo double resonance (REDOR) (*1*) remains one of the most powerful experimental approaches for quantifying the strength of heteronuclear dipole–dipole interactions under conditions of high-resolution solid-state NMR. The substantial potential of this technique for deriving unambiguous distance information is well-documented in the literature, in particular for cases of isolated pairs of spin-$\frac{1}{2}$ nuclei, where the theoretical description is particularly simple (*2*). Extensions to more complex spin systems have also been discussed, both from theoretical and from experimental points of view. In particular, various authors have treated the dephasing of coherence associated with an observe-spin S in the dipolar fields of multiple spins I in some detail (*3–6*). In general, the plot of signal attenuation $\Delta S/S_0$ versus dipolar evolution time NT_r (number of rotor cycles times rotor period), the so-called REDOR curve, depends sensitively on the molecular geometry of the spin systems involved. To avoid these complications, Gullion and Pennington have proposed the θ-REDOR approach which reduces the multiple-spin problem to a two-spin problem on a probabilistic basis, but results in an attenuation of the overall effect (*7*). Alternatively, our detailed simulations of standard REDOR behavior in spin systems with multiple dipolar interactions have shown that in the limit of short dipolar evolution times the dependence of the REDOR curve on molecular geometry is minimized (*6*). The general necessity of including the homonuclear I–I dipole–dipole interactions into simulations of such REDOR curves was first pointed out by Goetz and Schaefer (*8*). Also, the special complications involved when extending the technique to spin systems including quadrupolar nuclei have been discussed (*9, 10*). A principal motivation for studying such effects in detail stems from the desire of quantifying dipolar couplings in systems of unknown spin order and geometry, such as are frequently encountered in disordered inorganic systems and glasses. Indeed, the principal utility of REDOR to provide qualitative and semi-quantitative structural information in glasses has been independently demonstrated in several recent studies (*11–16*).

Most recently, we have shown that also for multiple-spin systems involving quadrupolar nuclei the initial parts of REDOR curves (data range $0 \leq \Delta S/S_0 \leq 0.3$) can be conveniently analyzed in terms of van Vleck's second moment information, even if the order and geometry of the spin system is completely unknown (*14*). In practice, however, the significance of any REDOR analysis largely depends on the fidelity of the experimental REDOR curves. There are imperfections such as finite pulse lengths, radiofrequency (RF) inhomogeneities, and drifts, as well as resonance offset effects, all of which effectively produce pulse-angle missets. The generally accepted best-effort approach for accounting for such imperfections is to calibrate the method on the basis of model compounds in which the dipole–dipole coupling constants are directly calculable from crystallographic information. Using this strategy, we have recently extracted some valuable infor-

[1] To whom correspondence should be addressed.

1090-7807/00 $35.00

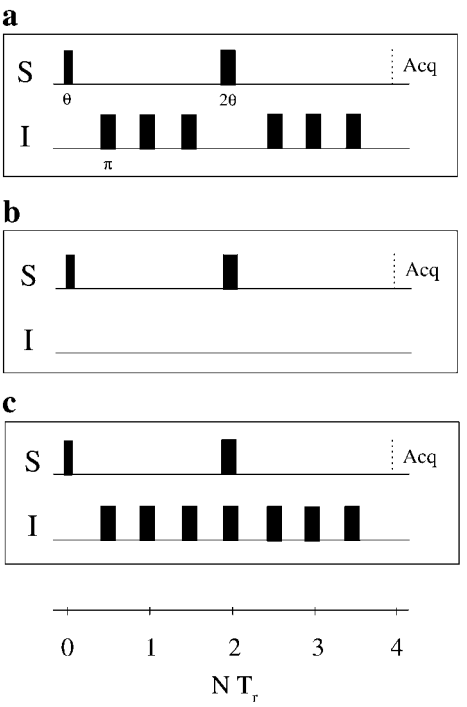

FIG. 1. Pulse sequences used within this study. Pulse sequences (a) and (b) constitute the ordinary REDOR experiment. Pulse sequence (c) serves to provide an empirical correction for pulse imperfection, abbreviated as the dummy echo sequence in the text.

mation on intermediate range structure in sodium aluminoborate glasses from REDOR data (*14*). Still, the question remains as to what extent calibration factors determined for model compounds are applicable to unknown systems, in which the spin dynamics (spectral dispersion, magnitude of dipolar and quadrupolar interactions, etc.) may or may not be comparable. In the present contribution, we demonstrate a simple compensation method that significantly improves the fidelity of REDOR data and lends itself to the reliable measurement of second moments without the need for external calibration. We will at first establish the method by numerical simulations and subsequently test it on some crystalline phosphates, including $Al(PO_3)_3$, $AlPO_4$, $[AlPO_4]_{12}(C_3H_7)_4NF$, and Na_3PO_4. The results obtained delineate the conditions under which this technique can be successfully applied to amorphous systems.

BACKGROUND

REDOR NMR. The pulse sequences shown in Figs. 1a and 1b constitute the REDOR experiments commonly carried out for the measurement of heteronuclear dipole–dipole coupling constants. We will call the sequences of Figs. 1a and 1b the REDOR sequence and the spin-echo sequence, respectively. If, as in the present application, dipole–dipole couplings between spin-$\frac{1}{2}$ nuclei (^{31}P) and quadrupolar nuclei (^{27}Al or ^{23}Na) are to be measured, the quadrupolar spin species is generally chosen for signal observation (*S* channel) (*17*). This choice eliminates systematic errors arising from ill-defined π pulse lengths due to distributions of nutation frequencies in powder samples (*18*): Provided that proper phase cycling is implemented, the procedure ensures that only nuclei subjected to the desired coherence pathway of a Hahn spin echo sequence contribute to the signal. This echo signal suffers attenuation by the 180° pulses of the *I* channel, the extent of which depends on the dipolar evolution time NT_r and the strength of the heterodipolar interaction. Assuming negligible homodipolar interactions among *I* spins, the REDOR fraction $\Delta S/S_0 = (S_0 - S)/S_0$ is given by

$$\frac{S_0 - S}{S_0} = 1 - \frac{1}{8\pi^2}\int \prod_{j=1}^{n} (\cos \Theta_j) d\Omega. \qquad [1]$$

Here S and S_0 are the echo intensities measured by the pulse sequences shown in Figs. 1a and b, Ω is the solid angle for powder averaging; Θ_j describes the dipolar dephasing associated with a particular dipolar vector $S–I_j$, which is a function of NT_r, dipolar coupling constants, and the relative orientation of $S - I_j$ with respect to a reference frame.

Dummy echo sequence. The pulse sequence shown in Fig. 1c plays the key role in our proposed experimental strategy. This pulse sequence is identical to that of Fig. 1a except for the presence of an additional π pulse on the *I* channel in the middle of the overall dipolar evolution period. The effect of this additional pulse is to keep the sign of the heteronuclear dipole–dipole interactions unchanged in the middle of the evolution period. As a consequence, the dipolar dephasings in the first half and second half of the evolution period become identical in magnitude but opposite in sign (*19*), leading to the result that the echo intensities are identical for the pulse sequences shown in Figs. 1b and 1c under perfect experimental conditions. In practice, however, the pulse sequence of Fig. 1b is a lot more robust and less susceptible to pulse imperfections than those of Figs. 1a and 1c. In fact, the echo intensity measured by the latter two sequences is significantly affected by experimental imperfections such as finite pulse width and RF inhomogeneity (*vide infra*). For ease of discussion, we call this pulse sequence (Fig. 1c) the "dummy echo" sequence and denote the associated echo intensity as S'.

EXPERIMENTAL

Sample preparation and characterization. $Al(PO_3)_3$ and $AlPO_4$ (a mixture of polymorphs: low-cristobalite and berlinite) were purchased from ALFA and dried at 125°C before use. $[AlPO_4]_{12}(C_3H_7)_4NF$ was a gift from Professor Ferdi Schüth at Max-Planck-Institut für Kohlenforschung and its structure has been described in the literature (*20*). Na_3PO_4 was prepared by solid-state reaction of Na_2CO_3 and $Na_4P_2O_7$ using a previously reported procedure (*21*). The samples were characterized by standard ^{27}Al and ^{31}P MAS-NMR spectroscopy, reproducing the re-

sults reported in the literature (*20, 22, 23*). The ^{27}Al and ^{23}Na TQMAS methods (*24*) were used to extract the quadrupolar parameters of Na_3PO_4, $AlPO_4$, and $[AlPO_4]_{12}(C_3H_7)_4NF$. In accordance to the finding of Fyfe *et al.* we observed both four- and six-coordinated aluminum sites for $[AlPO_4]_{12}(C_3H_7)_4NF$, indicating the presence of water molecules (*25*).

Solid-state NMR experiments. Solid-state NMR experiments were carried out at 130.3, 132.3, and 202.5 MHz for ^{27}Al, ^{23}Na, and ^{31}P, respectively, on a Bruker DSX 500 spectrometer, equipped with a 4-mm Bruker double resonance probe. The RF mutation frequencies employed for the ^{27}Al, ^{23}Na, and ^{31}P spins were 27.7, 41.6, and 135 kHz, respectively, measured on liquid samples. Saturation combs were applied before the relaxation delays for all REDOR experiments except for the $[AlPO_4]_{12}(C_3H_7)_4NF$ measurements. Relaxation delays were adjusted to 1.5 to 5 s. Typically, 128 transients were accumulated for each measurement. The isotropic chemical shifts of ^{27}Al, ^{23}Na, and ^{31}P were referenced to 1 M $AlCl_3$, 1 M NaCl, and 85% H_3PO_4 solutions, respectively. REDOR pulse sequences shown in Fig. 1 were used in conjunction with the *XY*-8 phase alternation scheme (*26*). Samples were packed into the middle $\frac{1}{3}$ of the rotor volume to optimize RF homogeneity. Phase cycling of 16 steps for spin-echo measurement was employed for the observe channel (*27*). Optimum π pulses for the decoupling channel were set by maximizing the REDOR difference signal ΔS at a chosen dephasing time. Spinning speeds at the magic angle were stabilized within 2 Hz.

Numerical simulations. REDOR simulations of SI_2 systems, taking the geometry of an equilateral triangle (sides of 3-Å length), were carried out using the SIMPSON package developed by Bak and Rasmussen (*28*). This package is a general computer routine applicable to virtually all kinds of solid-state NMR experiments. The evolution of the density matrix under time-dependent internal Hamiltonians is calculated for incrementally small steps during which the Hamiltonian is considered time-independent. For our simulations the maximum time step (max dt) over which the Hamiltonian is approximated to be time-independent was set to 1 μs. A powder averaging scheme containing 320 REPULSION angles (*29*) (alpha and beta) and 36 gamma angles was chosen. Simulations were done on the basis of the pulse sequences shown in Fig. 1. Finite pulse widths were assumed, and experimental imperfections were mimicked in terms of angle missettings from the ideal value of 180° for the I spins. All the calculated FIDs contained negligible imaginary contributions and the initial amplitudes of the real parts were taken for REDOR analyses. Relaxation effects were ignored. Data convergence was checked by repeating selected calculations using smaller max dt and more extensive powder averaging schemes.

RESULTS AND DISCUSSION

Effects of homonuclear dipole–dipole interactions. The chosen $^{13}C(^{31}P)_2$ equilateral three-spin system is characterized by sizable heteronuclear and homonuclear dipole–dipole coupling constants of comparable magnitude (453 and 731 Hz, respectively). Figure 2 demonstrates the effect of homonuclear dipole–dipole interactions to REDOR curves in this system. In accordance to the findings of Goetz and Schaefer (*8*), the homonuclear dipolar interaction has a significant influence at longer dipolar evolution times; however, it does not appreciably affect the REDOR curves within the data range $0 \leq \Delta S/S_0 \leq 0.3$ even at the condition of rotational resonance. The same conclusions were obtained in an analogous simulation of the dummy echo responses (sequence in Fig. 1c). Thus, we conclude that it is generally not necessary to consider the homonuclear I–I dipolar interaction in the simulations, when the analysis focuses on the initial REDOR data range $0 < \Delta S/S_0 < 0.30$. Therefore, all of the subsequent numerical calculations in the present study have been carried out without considering the effects of homonuclear dipole–dipole interaction. (In specific cases, the validity of this assumption was confirmed by appropriate repeat calculations in which the homonuclear couplings were explicitly included.)

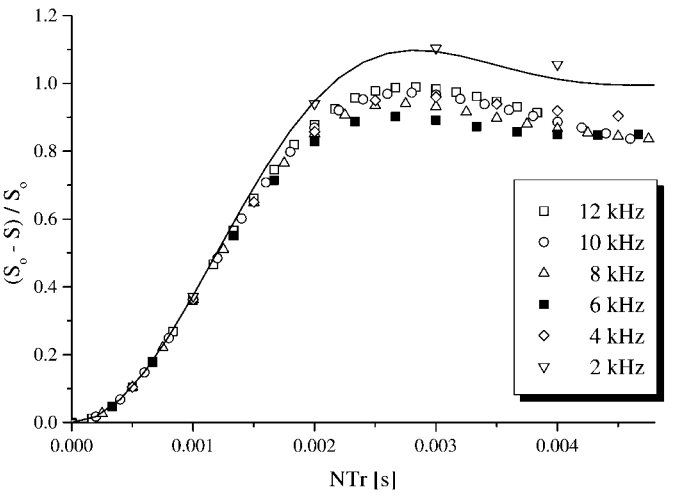

FIG. 2. Calculated $^{13}C\{^{31}P\}$ REDOR curves at different spinning speeds for a CP_2 system taking the geometry of a equilateral triangle. The simulations assume no ^{13}C chemical shift, a ^{31}P chemical shift difference of 6 kHz, and an RF field strength of 100 kHz. The solid line was calculated assuming no ^{31}P–^{31}P homonuclear interaction. Note that the curve calculated for a spinning speed of 6 kHz corresponds to the condition of rotational resonance.

Effects of finite pulse width and angle misset effects. Thus far, all the analytical expressions developed for the analysis of REDOR data assume that the pulses take the form of delta functions. Numerical calculations were carried out to assess the effects of finite pulse lengths and angle misset (as caused either by RF inhomogeneity or by resonance offsets) for the equilateral $^{13}C(^{31}P)_2$ spin system described above, based on heteronuclear dipole couplings only. The solid lines in Fig. 3 denote the ideal REDOR curves obtained for delta pulses. Figure 3a reveals that as the duty cycle (ratio of the pulse duration to rotor period) increases, the difference between the numerically

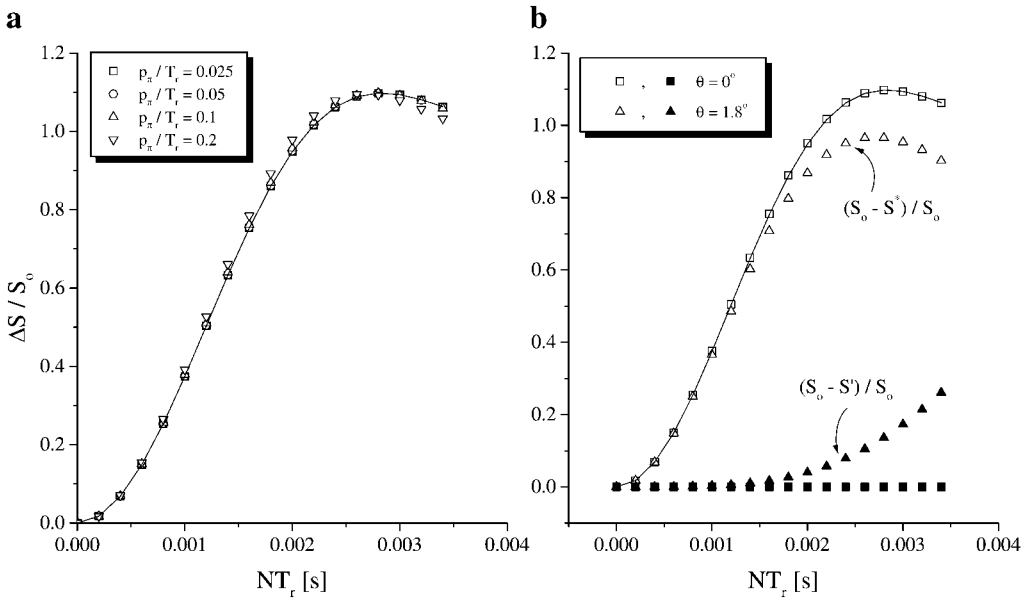

FIG. 3. Simulated difference signals under nonideal conditions for a $^{13}C(^{31}P)_2$ system as described in the text. Spinning speed was set at 10 kHz. The solid lines denote the REDOR curves calculated by the analytical equation for SI_n spin system (Eq. [1]). (a) Effects of pulse durations on the REDOR curve. p_π and T_r denote the π pulse duration and the rotor period, respectively. (b) Effects of pulse angle imperfections on REDOR and dummy echo difference signals. The angle θ indicates deviations from a perfect π pulse. The open and solid symbols denote the REDOR and the dummy echo difference signals, respectively. The duty cycle was set at 0.05. S^*, S_0, and S' denote the echo intensities measured by the pulse sequences of Figs. 1a, 1b, and 1c, respectively.

calculated and the ideal REDOR curves becomes more significant. Nevertheless, Fig. 3a illustrates that the delta-pulse approximation remains valid as long as the duty cycle is less than 10%. Similar results are also found by Schmidt and Vega (*30*). On the other hand, Fig. 3b shows that RF inhomogeneity will have a more significant effect on the REDOR curves. Deviations from perfect π pulses tend to reduce the REDOR fractions considerably (*31*). Qualitatively, this effect can be explained by the fact that imperfect π pulses only invert the heterodipolar coupling constants for a fraction of spin pairs so that the net dipolar dephasing becomes diminished. Significantly, we note that RF inhomogeneity also has substantial effects on the signals obtained by the dummy echo sequence. When the amplitudes of the dummy echoes S' are calculated as REDOR fractions of the spin-echo amplitude, i.e., $(S_0 - S')/S_0$, we observe a significant difference signal as the evolution time increases (Fig. 3b, solid symbols). This difference signal can be explained in terms of a probabilistic picture. Consider the dummy echo sequence in Fig. 1c. If we denote an imperfect π pulse as a pulse with flip angle $\pi + \theta$, the fraction of the spin system that undergoes perfect inversion would be equal to $[(1 + \cos\theta)/2]^n$ (n denotes the number of π pulses). This probability decreases as the number of inversion pulses increases, and hence a nonvanishing echo attenuation is observed.

Compensation for pulse inhomogeneity. Under ideal conditions, the dummy echo and the spin-echo pulse sequences are equivalent and would give identical echo signals for a pair of spin-$\frac{1}{2}$ species ($S' = S_0$). In real NMR experiments (finite pulse widths, RF inhomogeneity, etc.), our simulations show that the intensity of the dummy echo signal deviates from that of the spin-echo (see Fig. 3b). Note that the extent of the dummy echo attenuation is comparable to the deviation between the REDOR fractions with and without the effects of RF inhomogeneity, at least for the initial 30% regime. This effect suggests that we can compensate for imperfections in experimental REDOR curves by coadding both difference signals in some manner.

To evaluate this empirical correction quantitatively, in Fig. 4a we plot the normalized difference between the REDOR curves with and without the effects of RF inhomogeneity, $(S^* - S)/S_0$, against the corresponding dummy echo difference amplitudes, $(S_0 - S')/S_0$ (under ideal conditions $S' = S_0$). For small pulse angle missets ($<1°$), both the deviation and the compensation effects are negligible, but as the missets approach 5° the effects become noticeable. Only data corresponding to the initial 30% data range of the REDOR curve are included. Figure 4a illustrates that the magnitudes of the experimental deviation and the empirical compensation are indeed proportional to each other. Simple coaddition of both signals will produce no perfect compensation. From the slope of the least squares fit to the simulation data we can determine, however, that a full compensation can be accomplished if in the coaddition process the dummy echo difference signal is weighted by a calibration factor a, where the exact value of a depends on the ratio of $R = \pi$ pulse length/rotor period.

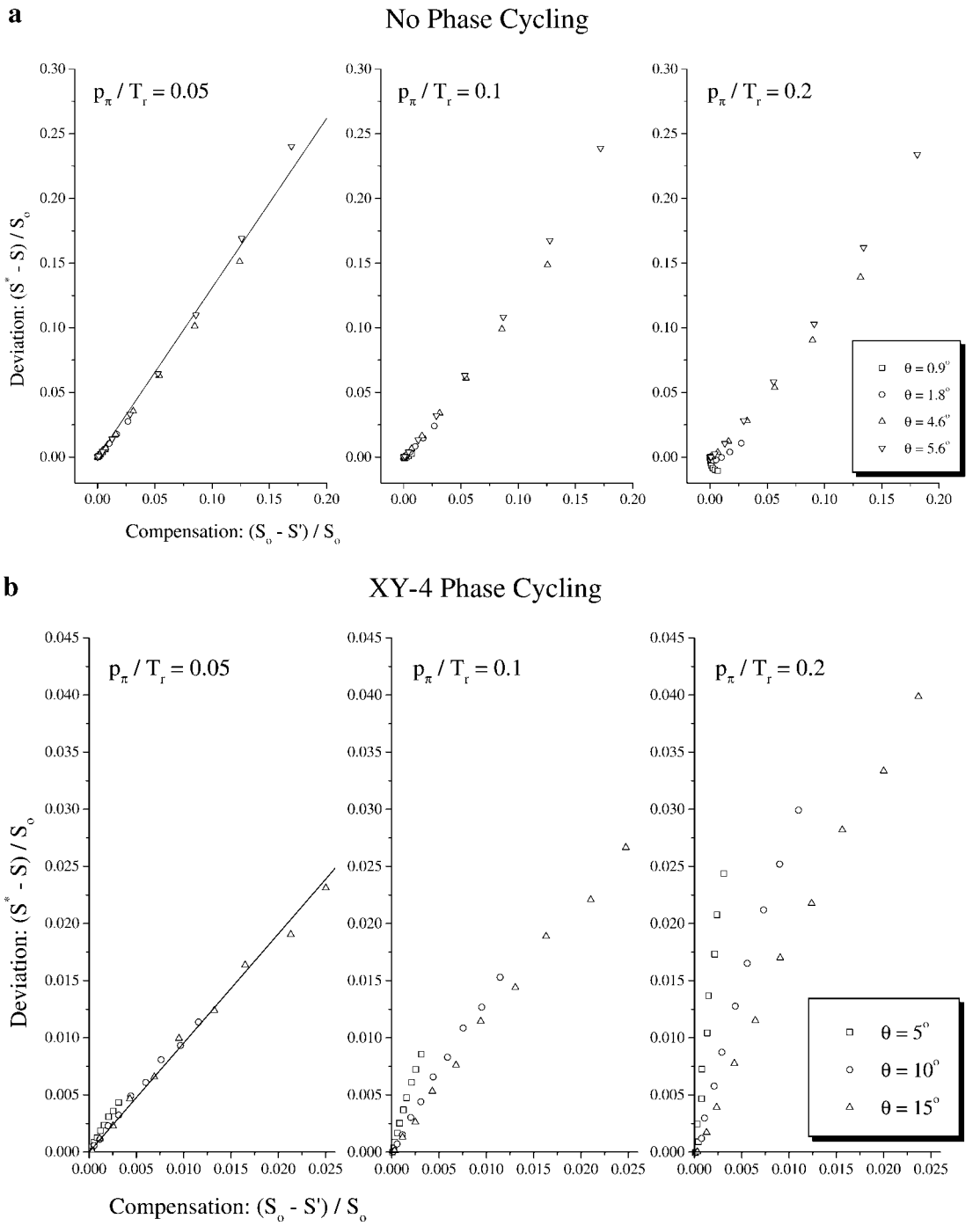

FIG. 4. Correlation of the REDOR deviation and the dummy echo difference signal for various extents of pulse angle imperfections. The solid line is a linear least squares fit to the data, whose slope is equal to the numerical factor a in Eq. [2] of the text. Simulations refer to values of R = pulse width/rotor period. (a) No phase cycling for the π pulse trains, $a = 1.31$. (b) XY-4 phase alternation, $a = 0.955$. (c) XY-8 phase cycling, $a = 1.35$.

$$\frac{S_0 - S^*}{S_0} + a\,\frac{S_0 - S'}{S_0} \approx 1 - \frac{1}{8\pi^2}\int \prod_{j=1}^{n} (\cos\Theta_j)\,d\Omega \qquad [2]$$

In experimental REDOR studies, it is a standard practice to phase cycle the π pulse trains in order to avoid the accumulation of flip-angle errors (*26*). To examine the effect of this phase cycling on our compensation scheme, additional numerical simulations were carried out. Comparing Figs. 4a and 4b, it is obvious that a simple XY-4 phase cycling of the π pulses greatly reduces the deviation of the REDOR data and extends

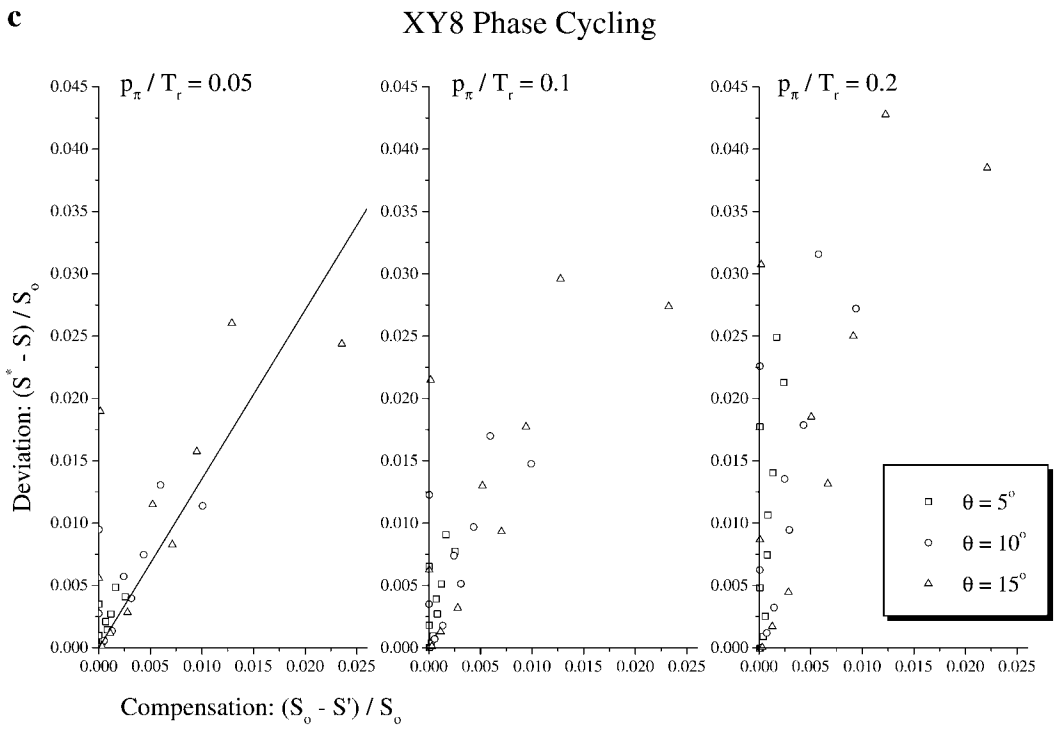

FIG. 4—*Continued*

the utility of our approach for a substantially larger flip-angle error (15°). In Fig. 4c, however, it is astonishing to find that the simulation results corresponding to the *XY*-8 phase alternation scheme show a significant data scattering (Fig. 4c). Nevertheless, our compensation scheme remains valid at $R = 0.05$. Overall, the simulations of the present study indicate that a is always close to unity.

Demonstration of the method on inorganic phosphates. In this section we verify the utility of the aforementioned empirical correction by $^{27}Al\{^{31}P\}$ and $^{23}Na\{^{31}P\}$ REDOR measurements on several model compounds with known geometries, including $AlPO_4$ (*32*, *33*), $Al(PO_3)_3$ (*34*), $[AlPO_4]_{12}(C_3H_7)_4NF$ (*20*), and Na_3PO_4 (*21*). The NMR parameters of these compounds are summarized in Table 1. Based on the available structural information the REDOR curves were calculated by Eq. [1] for the four-coordinated Al sites in $AlPO_4$ and $[AlPO_4]_{12}(C_3H_7)_4NF$, for the six-coordinated Al sites in $Al(PO_3)_3$, and for the four- and six-coordinated Na sites in Na_3PO_4.

The uncorrected and corrected experimental REDOR curves measured at spinning frequencies of 10 and 12 kHz are shown in Fig. 5. The uncorrected curves correspond to the experimen-

TABLE 1
Summary of the NMR Parameters of the Model Crystalline Compounds

		$Al(PO_3)_3$	$AlPO_4$	$AlPO_4$-5[a]	Na_3PO_4
^{31}P	δ_{iso} [ppm]	−50.7	−24.8/−26.4	−30/−23[b]	13.8
^{27}Al	δ_{iso} [ppm]	−21.6	41.5	39.2[c]/15.8[d]	—
	SOQE[e] [MHz]	0.22	1.6	2.57/3.54	—
^{23}Na	δ_{iso} [ppm]	—	—	—	2.5/2.5/4.5/8.3/31.5
	SOQE [MHz]	—	—	—	2.85/2.50/3.20/1.99/3.55
Al-P_n		6	4	4	—
Na-P_n		—	—	—	4 and 6

[a] $[AlPO_4]_{12}(C_3H_7)_4NF$.
[b] Minor peak.
[c] AlO_4.
[d] AlO_6.
[e] Second-order quadrupolar effect defined as $e^2qQ/h(1 + \eta_Q^2/3)^{1/2}$.

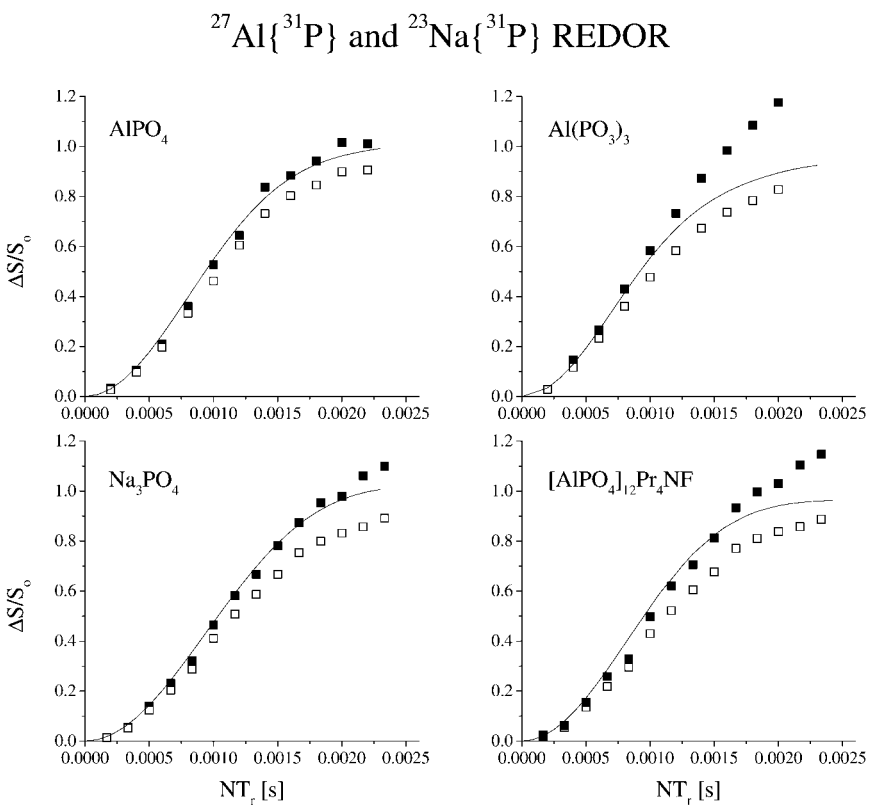

FIG. 5. Experimental and simulated REDOR curves for four crystalline model compounds. The theoretical REDOR curves were simulated under ideal conditions using Eq. [1], based on the known distance geometry within the closest interaction sphere (see text). The REDOR curve simulated for $AlPO_4$ and Na_3PO_4 is the average of the results calculated for the polymorphs and the multiple sites, respectively. Open symbols: uncorrected REDOR difference curve (raw experimental data). Filled symbols: compensated REDOR difference curve.

tal data obtained with the pulse sequences of Figs. 1a and 1b, while the corrected REDOR curves have been constructed according to Eq. [2]. The data are contrasted with simulated REDOR curves assuming perfect pulses (solid curves) and are calculated on the basis of the exact distance geometries present in the crystal structures of these compounds. The structures of the two polymorphs of $AlPO_4$, viz. berlinite and crystobalite, were used to calculate the average REDOR curve. The calculations included the distances to the four closest P-atoms, forming distorted tetrahedra around Al. For $Al(PO_3)_3$ only the closest six P-neighbors were taken into account, which form a distorted octahedron around Al. In Na_3PO_4, the average over the five sodium sites present was taken. Within their closest coordination spheres, four of these sodium sites are surrounded by four P-atoms, while one of them is octahedrally surrounded with P. For $(AlPO_4)_{12}Pr_4NF$ the calculation included the distances to the four closest P-atoms of the tetrahedral Al site.

Clearly, Fig. 5 reveals that despite our efforts of optimizing the RF homogeneity in our REDOR experiments, the standard REDOR data deviate substantially from the ideal behavior expected. The primary reason for these deviations is probably imperfect 180° pulses on the ^{31}P channel and/or limited RF homogeneity. Note, however, that application of the compensated sequence produces substantial improvement when the *XY*-8 phase cycling scheme was employed for the π pulse train in the *I* channel (Fig. 1). It appears that the compensation provided by the dummy echo sequence is larger than those predicted in our simulation results. Similar experimental observations were obtained for the *XY*-4 phase alternation scheme but the data improvement is less pronounced (data not shown). For a more precise analysis within the data range $0 < \Delta S/S_0 < 0.3$, we increase the number of data points in this region. The results compiled in Fig. 6 have been obtained by using different spinning frequencies, while still remaining within reasonable boundaries of duty cycle, such that the ensuing variations of R ($\approx$5%) do not produce large differences in the prefactor a. The solid curves show the appropriate multispin simulation (idealized octahedron for $Al(PO_3)_3$, tetrahedra for the other three compounds) resulting in the best fit with the experimental data. Experimental second moments extracted from these fits are summarized in Table 2 and are compared with the corresponding van Vleck values from the crystal structure. Note that for all four compounds the agreement lies within 10% of the true value. In contrast, extraction of second moments from the uncorrected experimental data (Eq. [1], Fig. 5) result in much larger deviations.

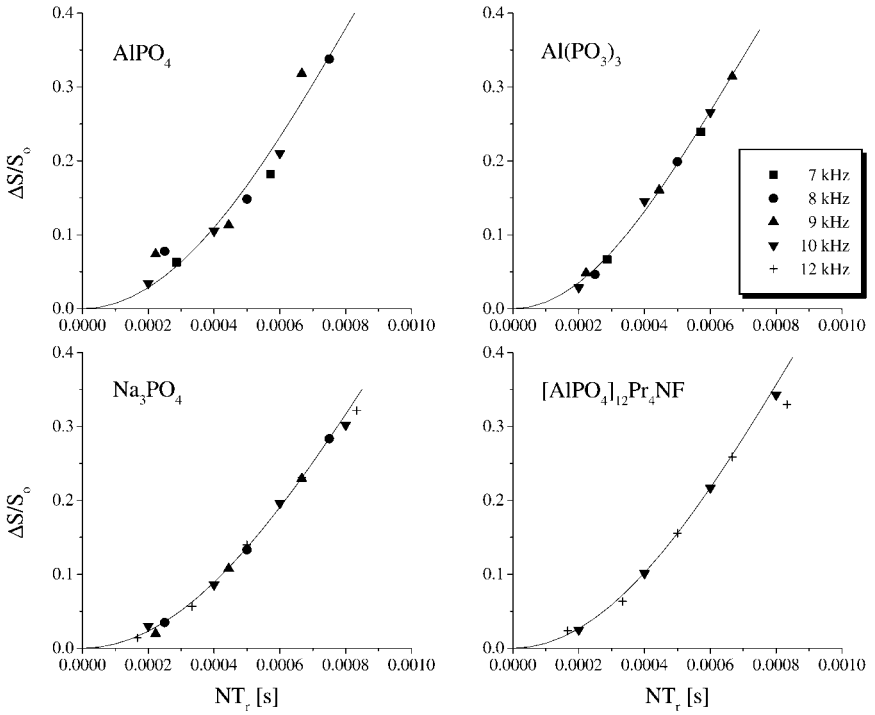

FIG. 6. Compensated REDOR curves measured on the model compounds within the data range $0 < \Delta S/S_0 < 0.30$. Solid curves represent best-fit multispin simulations producing the results summarized in Table 2. Idealized geometries (octahedron and tetrahedron) were assumed in the simulations.

CONCLUSIONS AND SUMMARY

We have demonstrated an experimental REDOR NMR method to yield reliable dipolar coupling information in multispin systems under nonideal experimental conditions. The simple compensation strategy (weighted coaddition of REDOR and DUMMY echo difference signals) used is easy to implement experimentally. We have tested this method successfully by numerical simulations and experiments on crystalline model compounds. The empirically corrected REDOR curve can then be analyzed by either assuming ideal geometry for a known coordination number or more generally by the second moment approach (*6*). In principle, the internal compensation described here obviates the use of calibration compounds to account for experimental imperfections. For possible applications to amorphous systems, this is a decisive benefit, since it removes the basic uncertainties as to whether (i) calibration factors determined for crystalline model compounds can be propagated and (ii) the experimental conditions of separate REDOR runs on different materials (to be compared with each other) were really identical. Application of this compensated REDOR NMR strategy to the quantitative structural description of sodium aluminophosphate glasses will be subject of a forthcoming publication.

TABLE 2
Summary of the Heterodipolar Second Moments of the Crystalline Models

M_2^{IS} [10^6 s^{-2}]	$Al(PO_3)_3$	$AlPO_4$	$AlPO_4$-5	Na_3PO_4
van Vleck[a]	6.46	5.64	5.57	4.68[b]
Expt, Eq. [1][c]	5.64 ± 0.05 (87%)[d]	4.56 ± 0.05 (81%)	3.98 ± 0.05 (71%)	3.92 ± 0.05 (84%)
Expt, Eq. [2][e]	6.66 ± 0.05 (103%)	5.40 ± 0.05 (96%)	5.05 ± 0.05 (91%)	4.37 ± 0.05 (93%)

[a] Calculated second moments using the van Vleck theory, considering the Al-P distances of the closest coordination sphere.

[b] Average value for the four- and six-coordinated Na sites.

[c] Uncorrected experimental data (Fig. 5) analyzed by multiple-spin REDOR simulation.

[d] Values in parentheses indicate the percentage of the van Vleck value.

[e] Corrected experimental data (Fig. 6) analyzed by multiple-spin REDOR simulation.

ACKNOWLEDGMENTS

We gratefully acknowledge the donation of $[AlPO_4]_{12}(C_3H_7)_4NF$ from Prof. Ferdi Schüth at Max-Planck-Institut für Kohleforschung. J.C.C.C. thanks the Alexander von Humboldt Foundation for a personal research stipend. Financial support of this work from the Deutsche Forschungsgemeinschaft (Grant Ec168/3-1), the Fond der Chemischen Industrie, and the Wissenschaftsministerium Nordrhein-Westfalen is most gratefully appreciated. We thank Dr. Michael Witschas for the analysis of the ^{23}Na MAS spectra of Na_3PO_4. We thank Mr. M. Bak for his kind assistance in our SIMPSON calculations.

REFERENCES

1. T. Gullion and J. Schaefer, Rotational-echo double-resonance NMR, *J. Magn. Reson.* **81,** 196–200 (1989).
2. Y. Pan, T. Gullion, and J. Schaefer, Determination of C–N internuclear distances by rotational-echo double-resonance NMR of solids, *J. Magn. Reson.* **90,** 330–340 (1990).
3. A. Naito, K. Nishimura, S. Tuzi, and H. Saitô, Inter- and intramolecular contributions of neighboring dipolar pairs to the precise determination of interatomic distances in a simple [^{13}C, ^{15}N]-peptide by ^{13}C, ^{15}N-REDOR NMR spectroscopy, *Chem. Phys. Lett.* **229,** 506–511 (1994).
4. C. A. Fyfe, A. R. Lewis, J. M. Chezeau, and H. Grondey, ^{19}F/^{29}Si distance determinations in fluoride-containing octadecasil from solid-state NMR measurements, *J. Am. Chem. Soc.* **119,** 12210–12222 (1997).
5. C. A. Fyfe and A. R. Lewis, Investigation of viability of solid-state NMR distance determinations in multiple spin systems of unknown structure, *J. Phys. Chem. B* **104,** 48–55 (2000).
6. M. Bertmer and H. Eckert, Dephasing of spin echoes by multiple heteronuclear dipolar interactions in rotational echo double resonance NMR experiments, *Solid State Nucl. Magn. Reson.* **15,** 139–152 (1999).
7. T. Gullion and C. H. Pennington, θ-REDOR: An MAS NMR method to simplify multiple coupled heteronuclear spin systems, *Chem. Phys. Lett.* **290,** 88–93 (1998).
8. J. M. Goetz and J. Schaefer, REDOR dephasing by multiple spins in the presence of molecular motion, *J. Magn. Reson.* **127,** 147–154 (1997).
9. C. Hudalla, H. Eckert, and R. Dupree, Structural studies of $ZrV_{2-x}P_xO_7$ solid solutions using ^{31}P–{^{51}V} and ^{51}V–{^{31}P} rotational echo double resonance NMR, *J. Phys. Chem.* **100,** 15986–15991 (1996).
10. L. Chopin, S. Vega, and T. Gullion, A MAS NMR method for measuring ^{13}C–^{17}O distances, *J. Am. Chem. Soc.* **120,** 4406–4409 (1998).
11. K. Herzog, B. Thomas, D. Sprenger, and J. Jäger, REDOR NMR: Approaching structural elucidation of hydrated layers in silicate electrode glasses, *J. Non-Cryst. Solids* **190,** 296–300 (1995).
12. L. van Wüllen, L. Züchner, W. Müller-Warmuth, and H. Eckert, ^{11}B{^{27}Al} and ^{27}Al{^{11}B} double resonance experiments on a glassy sodium aluminoborate, *Solid State Nucl. Magn. Reson.* **6,** 203–212 (1996).
13. J. C. C. Chan, M. Bertmer, and H. Eckert, Site connectivities in amorphous materials studied by double resonance NMR of quadrupolar nuclei: High resolution ^{11}B ↔ ^{27}Al spectroscopy of aluminoborate glasses, *J. Am. Chem. Soc.* **121,** 5238–5248 (1999).
14. M. Bertmer, L. Züchner, J. C. C. Chan, and H. Eckert, Short range order and site connectivities in sodium aluminoborate glasses: II. Site connectivities and cation distributions studied by rotational echo double resonance NMR spectroscopy, *J. Phys. Chem. B* **104,** 6541–6553 (2000).
15. L. van Wüllen, B. Gee, L. Züchner, M. Bertmer, and H. Eckert, Connectivities and cation distributions in oxide glasses: New results from solid state NMR, *Ber. Bunsenges. Phys. Chem.* **100,** 1539–1549 (1996).
16. L. van Wüllen, G. Schwering, and H. Eckert, Structure–property correlations in lithium phosphate glasses: new insights from ^{31}P ↔ ^{7}Li double resonance NMR, *Chem. Mater.* **12,** 1840–1846 (2000).
17. M. E. Smith and E. R. H. van Eck, Recent advances in experimental solid state NMR methodology for half-integer spin quadrupolar nuclei, *Prog. Nucl. Magn. Reson. Spectrosc.* **34,** 159–201 (1999).
18. D. Freude and J. Haase, Quadrupole effects in solid-state nuclear magnetic resonance, *NMR Basic Prin. Progress* **29,** 1–90 (1993).
19. T. Gullion, Measurement of heteronuclear dipolar interactions by rotational-echo, double-resonance nuclear magnetic resonance, *Magn. Reson. Rev.* **17,** 83–131 (1997).
20. S. Qiu, W. Pang, H. Kessler, and J.-L. Guth, Synthesis and structure of the $[AlPO_4]_{12}Pr_4NF$ molecular sieve with AFI structure, *Zeolites* **9,** 440–444 (1989).
21. E. Lissel, M. Jansen, E. Jansen, and G. Will, Bestimmung der Kristallstruktur von T-Na_3PO_4 mit Röntgen- und Neutronenpulvertechniken, *Z. Kristallogr.* **192,** 233–243 (1990).
22. D. Müller, E. Jahn, G. Ladwig, and U. Haubenreisser, High-resolution solid-state ^{27}Al and ^{31}P NMR: Correlation between chemical shift and mean Al-O-P angle in $AlPO_4$ polymorphs, *Chem. Phys. Lett.* **109,** 332–336 (1984).
23. D. Ehrt and C. Jäger, Investigations of solid state reactions of binary polyphosphate-fluoride systems by means of thermal analysis, x-ray diffraction and NMR spectroscopy, *Z. Phys. Chem. Neue Folge* **162,** 97–107 (1989).
24. L. Frydman and J. S. Harwood, Isotropic spectra of half-integer quadrupolar spins from bidimensional magic angle spinning NMR, *J. Am. Chem. Soc.* **117,** 5367–5368 (1995).
25. C. A. Fyfe, K. C. Wong-Moon, and Y. Huang, ^{27}Al/^{31}P solid-state NMR structural investigations of $AlPO_4$-5 molecular sieve, *Zeolites* **16,** 50–55 (1996).
26. T. Gullion, D. B. Baker, and M. S. Conradi, New, compensated Carr–Purcell sequences, *J. Magn. Reson.* **89,** 479–484 (1990).
27. A. C. Kunwar, G. L. Turner, and E. Oldfield, Solid-state spin-echo Fourier transform NMR of ^{39}K and ^{67}Zn salts at high field, *J. Magn. Reson.* **69,** 124–127 (1986).
28. M. Bak, J. T. Rasmussen, and N. C. Nielsen, Simpson version 1.0.0pre8, 40th Experimental NMR Conference, February 28–March 5, 1999, Orlando, FL, Poster Number 198.
29. M. Bak and N. C. Nielsen, REPULSION, a novel approach to efficient powder averaging in solid-state NMR, *J. Magn. Reson.* **125,** 132–139 (1997).
30. A. Schmidt and S. Vega, The transition amplitudes of centerband and sidebands in NMR spectra of rotating solids, *Isr. J. Chem.* **32,** 215–230 (1992).
31. T. Gullion, Introduction to rotational-echo, double-resonance NMR, *Concept Magn. Reson.* **10,** 277–289 (1998).
32. R. C. L. Mooney, The crystal structure of aluminum phosphate and gallium phosphate, low-cristobalite type, *Acta Crystallogr.* **9,** 728–734 (1956).
33. H. N. Ng and C. Calvo, X-ray study of the α-β transformation of berlinite $AlPO_4$, *Can. J. Phys.* **54,** 638–647 (1976).
34. L. Pauling and J. Z. Sherman, The crystal structure of aluminum metaphosphate, $Al(PO_3)_3$, *Z. Kristallogr.* **96,** 481–487 (1937).